Numerical Analysis of Dielectric Post-Wall Waveguides and Band-Pass Filters

Elguja Archemashvili, Vakhtang Jandieri, Hiroshi Maeda, Kiyotoshi Yasumoto, Jaromir Pistora, and Daniel Erni

Abstract – A functional dielectric post-wall waveguide (PWW) and a PWW-based band-pass filter that is formed by introducing specific arrangements of additional dielectric posts in the guiding region are numerically analyzed. In this preliminary study, the complex wavenumber of the dielectric PWW composed of dielectric rods as wall elements is rigorously calculated using our highly efficient full-wave formalism based on the lattice sums technique. Structural parameters of the dielectric PWW are properly chosen using a combination of our full-wave formalism, and a breeder genetic algorithm is employed as a global search heuristic to achieve a strong confinement of the electromagnetic fields with a relatively smaller number of layers in the lateral direction aiming at a realization of a compact functional device within the desired frequency range. After the structural parameters of the PWW are defined, a functional band-pass filter is realized. The S-parameters of the filter are calculated using the CST 3D EM simulation tool. It is expected that this study will find practical applications in device integration at millimeter-wave and terahertz frequencies—those at which metal rods used, for example, in conventional substrate-integrated waveguide schemes become too lossy and thus impair their guiding properties.

1. Introduction

Conventional rectangular waveguides developed several decades ago cannot be used for circuit and system integration because of their bulky mechanical and nonplanar nature. An alternative to conventional nonplanar guiding devices is the post-wall waveguide (PWW) [1–3]. A transversal view of a typical configuration of the PWW is shown in Figure 1. The electromagnetic fields of the PWW are confined in the lateral direction by periodic arrays of posts placed on both sides of the guiding channel. The height of the waveguide bounded by two metallic plates is much smaller than the wavelength, and the electromagnetic field does not change in the vertical direction. We have shown [4] that in the case of metallic (PEC) rods, a single array at both sides of the channel is usually enough to provide strong field confinement and guiding because the leakage of the guided waves is suppressed by the cutoff phenomenon between the adjacent PEC rods. However, at higher frequencies, the metals become increasingly lossy, and the dielectric materials start to play an important role [5]. Furthermore, the big technological step enabled by 3D printers allows a cheap and rapid prototyping by additive manufacturing of plastic materials and has attracted additional interest on the part of engineers for all-dielectric waveguide structures and integration schemes. However, the phenomenon of field confinement in the guiding region in the case of dielectric rods is still an open research issue, as the wall's elements are completely different from those of PEC rods. In the case of dielectric rods, the confinement is explicable by the electromagnetic band-gap behavior, similar to Bragg reflection in a periodic multilayered structure along the x-axis (Figure 1). As a result, the good confinement of the field could be achieved at the expense of a larger transversal extent of the device.

As a first step, we numerically analyze the PWW composed of periodically distributed dielectric circular rods as wall elements using our originally developed formalism based on the lattice sums technique [6–8], which enables us to calculate the propagation constant of complex modes (namely, the phase constant and the attenuation constant) for a wide class of periodic structures and electromagnetic band-gap structures in a very short computation time. Combining our full-wave formalism and a breeder genetic algorithm as an optimization technique, the geometrical parameters of PWW are properly tracked down to achieve a best possible confinement with a relatively small number N of PWW layers in the desired frequency range aiming at the realization of highly compact passive circuits. The developed formulation is numerically very fast [7, 8]; hence, it can be considered as one of the best-suited

Manuscript received 26 August 2020.

Elguja Archemashvili is with the Department of Electrical and Computer Engineering, Free University of Tbilisi, 0159 Tbilisi, Georgia; e-mail: earch16@freeuni.edu.ge.

Vakhtang Jandieri is with General and Theoretical Electrical Engineering (ATE), Faculty of Engineering, University of Duisburg-Essen, 47048 Duisburg, Germany; e-mail: vakhtang.jandieri@uni-due.de.

Hiroshi Maeda is with the Department of Information and Communication Engineering, Fukuoka Institute of Technology, Fukuoka 811-0295, Japan; e-mail: hiroshi@fit.ac.jp.

Kiyotoshi Yasumoto is with Kyushu University, Faculty of Information Science and Electrical Engineering, Professor Emeritus, Fukuoka 819-0395, Japan; e-mail: kiyoyasumoto@kag.bbiq.jp.

Jaromir Pistora is with the Nanotechnology Centre, VSB-Technical University of Ostrava, Ostrava–Poruba 708-33, Czech Republic; e-mail: jaromir.pistora@vsb.cz.

Daniel Erni is with General and Theoretical Electrical Engineering (ATE), Faculty of Engineering, and CENIDE—Center of Nanointegration Duisburg-Essen, University of Duisburg-Essen, 47048 Duisburg, Germany; e-mail: daniel.erni@uni-due.de.

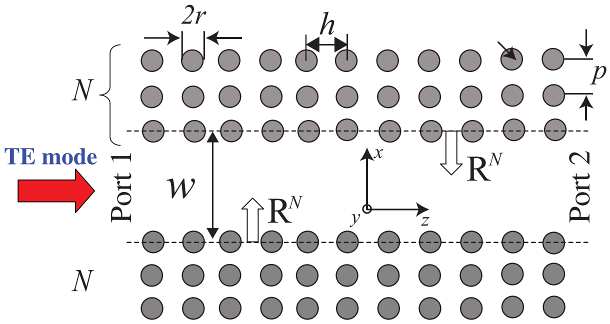

Figure 1. Transversal view of a dielectric PWW, where h is the period of the structure, w is the width of the waveguide, r is the radius of the dielectric rod, p is the distance between the layers, ϵ is the relative dielectric permittivity of the rod, and R^N is the generalized reflection matrix of the N-layered periodic structure. Guidance of a fundamental TE mode (E_y, H_x, H_z) injected in the dielectric PWW through Port 1 is considered.

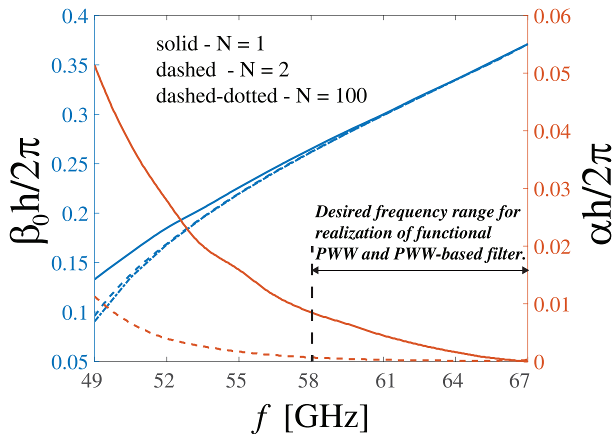

Figure 2. Normalized phase constant $\beta_0 h/2\pi$ (blue line) and normalized attenuation constant $\alpha h/2\pi$ (red line) of the lowest-order *TE* mode (E_y, H_x, H_z) for a one-layered (solid line) and a two-layered (dashed line) PWW composed of dielectric rods with $r = 0.353$ mm, $h = 1.96$ mm, $p = 1.96$ mm, $w = 3.92$ mm, and $\epsilon = 11.56$. The frequency dependence of $\beta_0\ h/2\pi$ for a multilayered $N = 100$ is also illustrated by a blue dashed-dotted line.

forward solvers in the framework of numerical structural optimization for the design of integrated PWW-based millimeter-wave/terahertz devices.

The phase constant and attenuation constant for one- and two-layered dielectric PWWs are rigorously analyzed. Near-field distributions are investigated and are showing promising results of strong field confinement in case of a two-layered waveguide structure when about 90% of the initial power is guided. A band-pass filter is realized by introducing specific arrangements of additional dielectric posts into the guiding channel. The S-parameters for the band-pass filter are calculated by means of CST Microwave Studio [9], demonstrating a realization of a compact functional passive filter based on a dielectric platform of PWW. Note that the effective method developed in [4], which can very effectively analyze the S-parameters of metallic PWW-based passive circuits, cannot be applied to the PWW with the dielectric rods. We believe that the proposed preliminary study could become valuable in the context of highly compact low-loss integrated schemes applicable to, for example, millimeter-wave/terahertz metrology and material characterization [10].

2. Formulation of the Problem

We choose a design goal, namely, to realize functional dielectric PWW and PWW-based passive filter within the frequency range 58 GHz $< f <$ 67 GHz (the desired frequency range is preliminarily defined, and it is marked in Figure 2). A guidance of the fundamental TE mode (E_y, H_x, H_z) is studied. The optimal geometrical parameters for the realization of the functional PWWs in the desired frequency bands can be effectively found based on a combination of our original EM solver (i.e., the full-wave formalism based on the lattice sums technique) and a breeder genetic algorithm [4, 11]. The high efficiency of the formalism has been already demonstrated in [4] for PWW with metal (PEC) rods as wall elements. The advantage of the method is related to the fast and accurate calculation of the lattice sums (i.e., semi-infinite series of the cylindrical functions) in the case of complex wavenumbers [7, 8]. The computation time to obtain the complex wavenumber per one frequency is about 0.07 s. This method provides a significant speedup over standard approaches (the details about a computation time of our method versus other numerical approaches are given in [4, 7, 8]). Our extensive numerical analysis using a breeder genetic algorithm has shown that the dielectric PWW having a width $w = 3.92$ mm, a radius of the dielectric cylindrical posts (as wall elements) of $r = 0.353$ mm, a period of $h = 1.96$ mm, $p = 1.96$ mm, and a relative dielectric permittivity of the rods of $\epsilon = 11.56$ (dielectric losses are taken into account using the data published in [12]) can be considered as one of the best candidates for our design goal. Our investigations have shown that the variations of a radius and a dielectric permittivity of the rods have a substantial effect on the transmittance in the dielectric PWW. Details on the use of the genetic algorithm for this kind of structure are not given here, and the interested reader may refer to [4].

The complex wavenumber k_z (from which the propagation constant is easily deduced) in the dielectric PWW at a fixed angular frequency ω can be calculated in the following form:

$$\mathrm{Det}[\mathbf{I} \pm \mathbf{W}(k_{z0}, w)\mathbf{R}^N(k_{z0}, w)] = 0 \qquad (1)$$

where $k_{z0} = \beta_0 + i\alpha$; β_0 and α are phase and attenuation constants, respectively; $\mathbf{R}^N(k_{z0}, \omega)$ denotes the generalized reflection matrix of the multilayered periodic structure calculated by a formalism developed in [6, 13]; $\mathbf{W}(k_{z0}, \omega)$ denotes the phase shift of each space harmonic in the guiding region along the x-axis; $\mathbf{I}$ is the unit matrix; and $\pm$ denotes odd and even modes, respectively. Figure 2 illustrates the dependence of both the normalized phase constant $\beta_0 h/2\pi$ (blue line) and the normalized attenuation constant $\alpha h/2\pi$ (red line) of

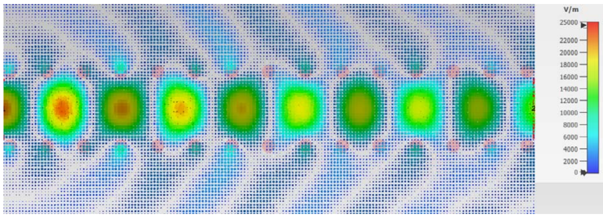

Figure 3. Near-field distribution of the electric field E_y of the fundamental mode for a one-layered dielectric PWW at the operating frequency $f = 62$ GHz.

the lowest-order mode (E_y, H_x, H_z) for one-layered (solid line) and two-layered (dashed line) dielectric PWWs within the frequency range 49 GHz $< f <$ 67 GHz. For comparison, the propagation constant for a waveguide structure with $N = 100$ is also shown for comparison by the blue dashed-dotted line (the attenuation constant is negligibly small because of the nearly perfect mode confinement). In the desired frequency range 58 GHz $< f <$ 67 GHz for the two-layered structure, the normalized attenuation constant varies between 0.0001 and 0.0005; thus, the corresponding PWW is applicable to the realization of the functional passive filters.

The near-field distribution of the electric field E_y of the fundamental mode for a one- and a two-layered dielectric PWW structure at 62 GHz is depicted in Figures 3 and 4, respectively. The total length of the structure is $15h$. At this frequency (62 GHz), the normalized attenuation constant is $\alpha\, h/2\pi = 0.0002$. The near fields are plotted by means of CST Microwave Studio [9]. Our numerical analysis has shown a strong field confinement in case of two-layered dielectric PWW when about 90% of the injected power is transmitted along the periodic dielectric waveguide structure. As for the one-layered structure, only about 35% of the initial power can be guided.

After the geometrical parameters of the PWW are defined, a band-pass filter is designed by introducing specific arrangements of additional dielectric posts (dielectric losses are taken into account using the data published in [12]) into the waveguide channel. Our goal was to design a filter 1) with $S_{11} < -20$ dB in the passband region and 2) with the resulting passband ripple about 0.15 dB yielding 3 dB bandwidths of 2 GHz. Because of a lack of an efficient technique for such kind of dielectric PWW-based filters, we were forced to do several time-consuming numerical tests by properly selecting a radius, a permittivity, and a distance between the elements to design a band-pass filter in the desired frequency range. A schematic view of a dielectric PWW-based filter formed by introducing five dielectric posts is shown in Figure 5. The frequency responses of the S-parameters are depicted in Figure 6 by the solid (S_{21}) and the dashed (S_{11}) lines, respectively. The S-parameters retrieved from CST show a distinct filter behavior from a functional band-pass filter structure based on a dielectric PWW. We succeeded in having $S_{11} < -20$ dB in the passband region; however, the bandwidth is slightly larger than we expected. We understand that a better solution could exist. In order to achieve the best filter characteristics in the desired frequency range, a development of the numerically fast full-wave formalism is required. Present research is therefore focusing on the development of an approach that is directly applicable to our efficient analysis formalism. It is expected to provide a

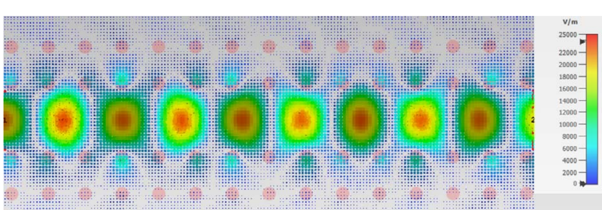

Figure 4. Near-field distribution of the electric field E_y of the fundamental mode for a two-layered dielectric PWW at the operating frequency $f = 62$ GHz.

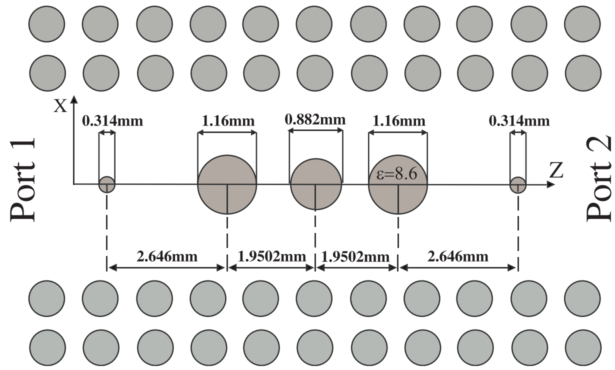

Figure 5. Schematic view of the dielectric PWW-based filter formed by additionally injecting the dielectric rods into the PWW.

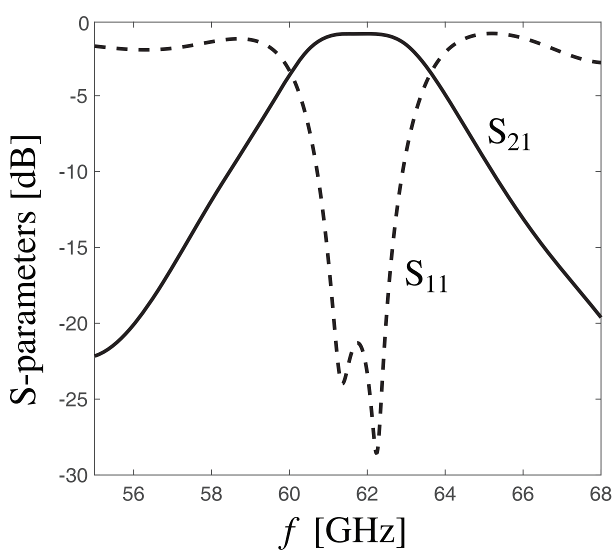

Figure 6. Frequency response of the S-parameters of the dielectric PWW-based filter shown in Figure 5.

significant speedup over the standard approaches. The method will be proposed in due course.

3. Conclusion

In this preliminary study, we have reported on the numerical investigations of the compact and functional dielectric PWW-based filter, which is potentially applicable also at terahertz frequencies, where the metallic rods are losing their intended properties due to the increasing losses. The PWW has been numerically studied, and its structural parameters have been properly defined based on our self-contained semi-analytical formalism in combination with a breeder genetic algorithm for a realization of the functional passive filter in a defined frequency range. The S-parameters of the designed band-pass filter formed by introducing additional dielectric posts inside the PWW have been calculated using the commercial CST software. Dielectric alternatives to integration concepts based on substrate integrated waveguides are particularly promising, especially in the upcoming realm of additively manufactured terahertz circuits.

4. Acknowledgments

This work was supported by the Deutsche Forschungsgemeinschaft (German Research Foundation)– TRR 196 MARIE under grant 287022738 (project M03). The work was supported by the Shota Rustaveli National Science Foundation of Georgia (SRNSFG) (grant number FR-19-4058).

5. References

1. J. Hirokawa and M. Ando, "Single-Layer Feed Waveguide Consisting of Posts for Plane TEM Wave Excitation in Parallel Plates," *IEEE Transactions on Antennas and Propagation*, **46**, 5, May 1998, pp. 625-630.
2. H. Uchiyama, T. Takenoshita, and M. Fujii, "Development of a 'Laminated Waveguide,'" *IEEE Transactions on Microwave Theory and Techniques*, **46**, 12, December 1998, pp. 2438-2443.
3. D. Deslandes and K. Wu, "Accurate Modeling, Wave Mechanisms, and Design Considerations of a Substrate Integrated Waveguide," *IEEE Transactions on Microwave Theory and Techniques*, **54**, 6, June 2006, pp. 2516-2526.
4. A. Akopian, G. Burduli, V. Jandieri, H. Maeda, W. Hong, A. Omar, K. Yasumoto, D. H. Werner, and D. Erni, "Efficient Analysis of Electromagnetic Scattering in Post-Wall Waveguides and Its Application to Optimization of Millimeter Wave Filters," *IEEE Open Journal on Antennas and Propagation*, **1**, August 2020, pp. 448-455.
5. N. Dolatsha, *Hybrid Integration of Millimeter Wave Circuits Based on Low-Loss Dielectric Waveguides*, PhD Thesis, ETH Zurich No. 21527, Zurich, Switzerland, 2013.
6. K. Yasumoto (ed.), *Electromagnetic Theory and Applications for Photonic Crystals*, Boca Raton, FL, CRC Press, 2005.
7. V. Jandieri, P. Baccarelli, G. Valerio, and G. Schettini, "1-D Periodic Lattice Sums for Complex and Leaky Waves in 2-D Structures Using Higher-Order Ewald Formulation," *IEEE Transactions on Antennas and Propagation*, **67**, 4, January 2019, pp. 2364-2378.
8. V. Jandieri, P. Baccarelli, G. Valerio, K. Yasumoto, and G. Schettini, "Modal Propagation in Periodic Chains of Circular Rods: Real and Complex Solutions," *IEEE Photonics Technology Letters*, **32**, 17, July 2020, pp. 1053-1056.
9. CST (Feb. 14, 2017). *Computer Simulation Technology GmbH*. [Online]. Available: https://www.cst.com.
10. MARIE – A collaborative research center on THz material characterization and localization funded by the Deutsche Forschungsgemeinschaft (DFG, German Research Foundation) – Project-ID 287022738 – TRR 196 MARIE (Projects M03, M02).
11. C. Hafner, J. Smajic, and D. Erni, "Simulation and Optimization of Composite Doped Metamaterials," in M. Rieth and W. Schommers (eds.), *Handbook of Theoretical and Computational Nanotechnology*, Vol. 8, Stevenson Ranch, CA, American Scientific Publishers, 2006, Chapter 11.
12. J. Baker-Jarvis, M. D. Janezic, B. Riddle, C. L. Holloway, N. G. Paulter, and J. E. Blendell, "Dielectric and Conductor-Loss Characterization and Measurements on Electronic Packaging Materials," *NIST Technical Note*, July 2001.
13. K. Yasumoto, H. Toyama, and R. Kushta, "Accurate Analysis of Two-Dimensional Electromagnetic Scattering From Multilayered Periodic Arrays of Circular Cylinders Using Lattice Sums Technique," *IEEE Transactions on Antennas and Propagation*, **52**, 10, October 2004, pp. 2603-2611.